The Cryosphere Discuss., 7, 943–973, 2013
www.the-cryosphere-discuss.net/7/943/2013/
doi:10.5194/tcd-7-943-2013

The Cryosphere Discussions
Open Access

The effects of additional black carbon on Arctic sea ice surface albedo: variation with sea ice type and snow cover

A. A. Marks and M. D. King

Department of Earth Sciences, Royal Holloway University of London, Egham, Surrey, TW20 0EX, UK

Received: 31 January 2013 – Accepted: 11 February 2013 – Published: 6 March 2013

Correspondence to: M. D. King (m.king@es.rhul.ac.uk)

Published by Copernicus Publications on behalf of the European Geosciences Union.

Abstract

Black carbon in sea ice will decrease sea ice surface albedo through increased absorption of incident solar radiation, exacerbating sea ice melting. Previous literature has reported different albedo responses to additions of black carbon in sea ice and has not considered how a snow cover may mitigate the effect of black carbon in sea ice. Sea ice is predominately snow covered. Visible light absorption and light scattering coefficients are calculated for a typical first year and multi-year sea ice and "dry" and "wet" snow types that suggest black carbon is the dominating absorbing impurity. The albedo response of first year and multi-year sea ice to increasing black carbon, from 1–1024 ng g^{-1}, in a top 5 cm layer of a 155 cm thick sea ice was calculated using the radiative transfer model: TUV-snow. Sea ice albedo is surprisingly unresponsive to black carbon additions up to 100 ng g^{-1} with a decrease in albedo to 98.7 % of the original albedo value due to an addition of 8 ng g^{-1} of black carbon in first year sea ice compared to an albedo decrease to 99.6 % for the same black carbon mass ratio increase in multi-year sea ice. The first year sea ice proved more responsive to black carbon additions than the multi-year ice. Comparison with previous modelling of black carbon in sea ice suggests a more scattering sea ice environment will be less responsive to black carbon additions. Snow layers on sea ice may mitigate the effects of black carbon in sea ice. "Wet" and "dry" snow layers of 0.5, 1, 2, 5 and 10 cm were added onto the sea ice surface and the snow surface albedo calculated with the same increase in black carbon in the underlying sea ice. Just a 0.5 cm layer of snow greatly diminishes the effect of black carbon on surface albedo, and a 2–5 cm layer (less than half the *e*-folding depth of snow) is enough to "mask" any change in surface albedo owing to additional black carbon in sea ice, but not thick enough to ignore the underlying sea ice.

1 Introduction

Changes in the surface albedo of sea ice have a crucial role in determining the magnitude of modern climate change (Barry, 1996; Brandt et al., 2005; Curry et al., 1995; Gardner, 2010; Perovich et al., 2002; Perovich and Polashenski, 2012) and can be caused by the addition of black carbon to sea ice (Grenfell et al., 2002; Jacobson, 2001; Light et al., 1998; Ledley and Thompson, 1986). Black carbon has a large absorption cross-section over shortwave (UV and visible) wavelengths (e.g. Mitchell, 1957; Highwood and Kinnersley, 2006; Hansen and Nazarenko, 2004; Jacobson, 2001; Ramanathan and Carmichael, 2008) and is potentially the second greatest contributor, by means of direct radiative forcing, to anthropogenic global warming after carbon dioxide (Jacobson, 2001; Ramanathan and Carmichael, 2008). The deposition of black carbon from the atmosphere on to sea ice causes a decrease in the albedo through increased absorption of downwelling solar radiation; potentially resulting in increased melting of sea ice. A loss of sea ice owing to melting causes a drastic decrease in planetary albedo as the large surface albedo of the sea ice is replaced with the small surface albedo of the ocean.

Black carbon is likely to be found in small quantities throughout sea ice due to direct entrainment from seawater (Suman et al., 1997; Dittmar, 2008) and from sediment inclusions where sea ice forms over shallow ocean shelves (Masiello, 1998; Middelburg and Nieuwenhuize, 1999). Black carbon may be concentrated in a layer at the sea ice surface due to atmospheric deposition and following overlying snow melt.

The effects of black carbon in snow have been widely researched (e.g. Chýlek and Ramaswamy, 1983; Warren, 1984; Warren and Wiscombe, 1985; Clarke and Noone, 1985; Warren and Clarke, 1990; Hansen and Nazarenko, 2004; Flanner et al., 2007; Doherty et al., 2010; Reay et al., 2012). Black carbon may reduce the albedo of snow and have a positive climatic radiative forcing effect, with Clarke and Noone (1985) showing black carbon in snow could reduce albedo by 1–3 %. The 2007 IPCC report quantified the possible positive forcing as $0.1 \pm 0.1\,\mathrm{W\,m^{-2}}$ (Solomon et al., 2007).

Research into black carbon in sea ice is much less extensive (Grenfell et al., 2002; Jacobson, 2004; Light et al., 1998; Ledley and Thompson, 1986) although research into sea ice properties is more significant (Perovich et al., 1998, 2002; Perovich, 2003, 2006; Light et al., 2008; Grenfell and Maykut, 1977). Grenfell et al. (2002) demonstrated an increase in summer ablation rate occurs if soot is concentrated near the sea ice surface by using a multilayer four-stream radiative-transfer model to investigate the effect of varying mass ratios and vertical distribution of soot on albedo of the sea ice surface, between wavelengths of 350–2750 nm. Jacobson (2004) suggest that $25\,\mathrm{ng\,g^{-1}}$ of black carbon can reduce surface albedo of sea ice at a wavelength of 550 nm to 97.9 % of the original value. Using a one-dimensional radiative-transfer model Jacobson (2004) investigated the effect of black carbon on albedo and emissivity of snow and sea ice using black carbon concentrations in sea ice of $0–500\,\mathrm{ng\,g^{-1}}$ and a wavelength range from 200–1000 nm. Light et al. (1998) suggest $150\,\mathrm{ng\,g^{-1}}$ of soot included within sea ice can lead to an albedo decrease to 70 % of the original value. Light et al. (1998) investigated effects of sediment particles in sea ice on sea ice albedo, at wavelengths from 400–1000 nm, relative to the effect of one concentration of soot particles, using a four-stream radiative-transfer model. Ledley and Thompson (1986), using a one dimensional thermodynamic sea ice model, showed that soot deposition on sea ice following a nuclear disaster could significantly decrease the albedo of sea ice, resulting in a decrease in sea ice thickness and possibly leading to an increase in ice free conditions. Black carbon in sea ice has recently been added to global climate models; Goldenson et al. (2012) used the Community Earth System Model Version 1 (CESM1) to model the forcing due to black carbon and dust in snow and sea ice, and Holland et al. (2012) utilised the Community Climate System Model 4 to investigate the impact of melt ponds and aerosols (black carbon and dust) on Arctic sea ice. Goldenson et al. (2012) suggest black carbon could cause a decrease in Arctic sea ice thickness of 0.34 m in September, while Holland et al. (2012) conclude that black carbon and dust causes an annual average $0.2\,\mathrm{W\,m^{-2}}$ increase in shortwave absorption in Arctic sea ice.

Black carbon in sea ice will influence surface albedo differently depending on individual sea ice properties. Light et al. (1998); Grenfell et al. (2002); Jacobson (2004) suggest that for a black carbon increase in sea ice from 0–100 ng g^{-1} albedo at a wavelength of 500 nm will decrease to 73 %, 99 % and 92 % of the original values respectively. Different sea ice properties were used for some of these studies. Sea ice physical properties, including scattering, absorption and density, will affect surface albedo of sea ice and thus impact the extent to which black carbon will affect sea ice albedo. Physical properties of sea ice are determined by the presence of air bubbles, brine inclusions and also ice interior structure (Perovich, 2003).

Snow cover on sea ice may mitigate the effect of black carbon in sea ice on the surface albedo. Snow cover on sea ice is commonly up to a few tens of centimetres thick (Weeks, 2010). Light penetrates snow and underlying sea ice (e.g. King and Simpson, 2001; King et al., 2005) thus the optical properties of sea ice (i.e. black carbon content) will strongly influence snow surface albedo. Where a thin snow cover is present black carbon in sea ice may potentially lower the albedo of the snow surface overlying sea ice, leading to increased snow melting. The effects of a snow cover on sea ice containing black carbon need to be fully understood in order to understand the degree to which black carbon in sea ice may be climatically important. Warren and Wiscombe (1980) calculated that 2 cm liquid equivalent of snow is enough for albedo to be semi-infinite or "optically thick" (within 1 % of the albedo of an infinitely thick snowpack) this equates to 8 cm of new, "fluffy" snow, or 20 cm of old, compacted snow. France et al. (2011) suggest a snowpack needs to be greater than 3–4 *e*-folding depths (~ 10–20 cm) before it is optically thick enough for its albedo to be uninfluenced by the underlying surface. However these calculations were assuming snow on a dark surface and the case of snow on sea ice will be different. Warren and Wiscombe (1980) and Brandt et al. (2005) briefly consider the effect of snow on the albedo of sea ice with Brandt et al. (2005) suggesting that just 3 cm of snow on sea ice may be optically thick and therefore black carbon in sea ice would no longer be detectible in the snow surface albedo.

The work presented here has two aims. To establish the response of the surface albedo of different sea ice types to black carbon in sea ice. Secondly, to establish how a snow cover over sea ice mitigates the influence of black carbon in sea ice on the surface albedo, and how the effect varies with snow and sea ice type – an effect that to the authors knowledge has not previously been quantified.

2 Method

A coupled atmosphere-snow-sea ice radiative-transfer model (TUV-snow) was utilised to perform radiative-transfer calculations of irradiance in and above two Arctic sea ice types which were described by the fieldwork of Grenfell and Maykut (1977). The technique for determining the albedo response of the different sea ice types to black carbon is described in Sect. 2.1. To establish the extent to which a snow cover will mitigate the albedo effect of black carbon in sea ice two different Arctic snow types (also described by Grenfell and Maykut, 1977) were placed in increasingly thick layers overlying the original sea ice in the TUV-snow model; this process is also described in Sect. 2.1. The TUV-snow model uses the DISORT code (Stamnes et al., 1988) and is described in detail by Lee-Taylor and Madronich (2002). The model parameterizes sea ice and snow optical properties using only an asymmetry factor, g, a wavelength independent scattering cross-section, σ_{scatt}, a wavelength dependant absorption cross-section, $\sigma^{+}_{\mathrm{abs}}$, and snow/sea ice density. Values of scattering and absorption cross section for the snow and sea ice types modelled were obtained from albedo and *e*-folding depth data provided by Grenfell and Maykut (1977) using a technique described in Sect. 2.2. The technique also enables the identification of black carbon as the main absorbing impurity in sea ice and enables the mass ratio of black carbon in sea ice to be estimated.

2.1 Modelling albedo change in sea ice and snow on sea ice with increasing black carbon

Firstly, changes in sea ice surface albedo with a change in black carbon mass ratio in a 5 cm surface layer of the sea ice were calculated. Albedo was calculated as the ratio of upwelling to downwelling irradaince ($\frac{\mathrm{Irr_{up}}}{\mathrm{Irr_{down}}}$). Two different sea ice types (based on fieldwork of Grenfell and Maykut, 1977) were considered to establish the differing response of albedo to increased black carbon in different sea ice types.

1. A first year ice: a 155 cm blue sea ice layer with additional black carbon in the top 5 cm.
2. A multi-year ice: a 150 cm blue sea ice layer, with a top 5 cm granular white ice layer containing additional black carbon.

Grenfell and Maykut (1977) state that the melting multi-year ice observed in the Arctic basin was typically bluish-white in colour (similar to the first year blue ice) with a decomposed layer at the surface ranging from 2–15 cm thick, which is our granular white ice layer. Therefore sea ice (1) represents a typical first year sea ice, while sea ice (2) represents a typical multi-year sea ice.

Secondly, surface albedo of two different snow covers overlying the multi-year and first year sea ice were studied to observe the extent to which change in black carbon mass ratio in the underlying sea ice could be detected in the surface albedo of snow. The depth of snow cover which will mitigate the effect that black carbon in sea ice has on surface albedo is also calculated. Where a snow cover was present the albedo at the top of the snow layer was calculated. The albedo of an optically thick layer of snow on sea ice will have optical properties of snow, however the albedo of a thin layer of snow will be influenced by the optical properties of the sea ice below it. Snow coverings of 0.5, 1, 2, 5, and 10 cm of a "dry" and "wet" snow were added to both sea ice types. The "dry" and "wet" snows are based on the optical properties of "dry" and "wet" snowpacks described in Grenfell and Maykut (1977).

The snow and sea ice formations are in Fig. 1, black carbon mass ratio of 0, 1, 2, 4, 8, 16, 32, 64, 128, 256, 512, 1024 ng g^{-1} were used. Note the black carbon is additional to any already present. Therefore total light absorption in the layer containing additional black carbon is represented by Eq. (1).

$$\sigma_{\mathrm{abs}}(\lambda) = \sigma^{\mathrm{ice}}_{\mathrm{abs}}(\lambda) + \sigma^{+}_{\mathrm{abs}}(\lambda) + \sigma^{\mathrm{BC}}_{\mathrm{abs}}(\lambda) \quad (1)$$

where, $\sigma^{\mathrm{ice}}_{\mathrm{abs}}(\lambda)$, is absorption cross-section for ice, $\sigma^{+}_{\mathrm{abs}}(\lambda)$, is absorption cross-section due to impurities already present in the snowpack, or in the sea ice, $\sigma^{\mathrm{BC}}_{\mathrm{abs}}(\lambda)$ is absorption by additional black carbon and, λ, is wavelength of light.

The sea ice below the uppermost 5 cm layer had no additional black carbon, and the snow layer, where present, was also modelled with no additional black carbon. Additional black carbon was placed in only a 5 cm layer at the top of the sea ice as atmospheric deposition and surface snow melt concentrate black carbon at the top of the sea ice.

The absorption spectrum for black carbon in an ice matrix is determined by a Mie calculation using the method outlined by Warren and Wiscombe (1980). The wavelength independent refractive index of black carbon particles was chosen as 1.8–0.5i, with a diameter of 0.2 µm and density of 1 g cm^{-3}; these values were justified by Warren and Wiscombe (1985, 1980). The wavelength dependant refractive index of the surrounding ice was taken from Warren and Brandt (2008).

Calculations were undertaken at wavelengths 400–700 nm, using an eight-stream radiative-transfer calculation with a pseudo-spherical correction (Lee-Taylor and Madronich, 2002). The atmosphere had an ozone column of 300 Dobsons with no aerosol. A wavelength independent under-ice albedo was used of 0.1 and the Earth–Sun distance was set to 1 AU. Diffuse sky conditions were used throughout the work by placing cumulus clouds in the model at a 1 km altitude, with an optical depth of 32, an asymmetry parameter of 0.85 and a single scattering albedo of 0.9999. Diffuse sky conditions were used to be independent of solar zenith angle. The albedo of sea ice and snow depend on the solar zenith angle but are not dependant on the absolute

irradiance of incident radiation. The TUV-snow model has been previously used for coupled atmosphere-sea ice radiative-transfer calculations (e.g. King et al., 2005), multiple times for coupled atmosphere-snow calculations (e.g. Beine et al., 2006; France and King, 2007; France et al., 2010b,a, 2011, 2012), and validated in artificial laboratory snow experiments (Phillips, 2005). The work presented here is the first time the TUV-snow model has been configured to a coupled atmosphere-snow-sea ice system.

2.2 Obtaining scattering and absorption cross-section values for snow and sea ice

Grenfell and Maykut (1977) conducted measurements of light extinction coefficient (optical wavelengths 400–800 nm) and albedo (optical wavelengths 400–1000 nm) for melt ponds, snow on sea ice, and bare sea ice on first year sea ice near Point Barrow, Alaska, and on multi-year ice near Fletcher's Ice Island in the Beaufort Sea. Two sea ice types and two snow types were selected from the data of Grenfell and Maykut (1977) as representative for the study presented here and are described in the previous section and in Table 1 and Fig. 1. Using the albedo and extinction coefficient data of the two sea ice types and two snow types, see Table 1, scattering, ($\sigma_{\mathrm{Scatt}}(\lambda)$), and absorption ($\sigma^{+}_{\mathrm{abs}}(\lambda)$), cross-section values were calculated using a method developed and described in detail by Lee-Taylor and Madronich (2002) and very briefly described here. Radiative-transfer calculations of albedo and *e*-folding depths for a range of combinations of scattering and absorption cross-section values were undertaken using the TUV-snow model. For the radiative-transfer calculations the sea ice was modeled as 1 m thick, with 24 layers and the atmosphere was aerosol free. The measurement date was used to calculate earth-sun distance. Sky conditions, asymmetry factor (g), sea ice/snow density and solar zenith angle were all dependent on the sea ice/snow modelled, values for these are shown in Table 1. The albedo and *e*-folding depth are then interpolated to find unique values for scattering and absorption at a specific wavelength that concur with Grenfell and Maykut (1977) field measurements of both albedo and extinction coefficient, where *e*-folding depth, ϵ, is related to extinction coefficient, κ, by

Eq. (2). The technique has previously been used for sea ice by King et al. (2005) and for snow by France et al. (2011, 2012).

$$\epsilon = \frac{1}{\kappa} \tag{2}$$

The calculated scattering values for each of the sea ice and snow types were assumed wavelength independent (Lee-Taylor and Madronich, 2002); these calculated values of scattering cross-section are also shown in Table 1. However the calculated absorption cross-section values for each sea ice and snow type were wavelength dependant; these are shown in Fig. 2.

3 Results

The results section will describe how the effect of additional black carbon on surface albedo in a surface layer of sea ice varies with sea ice type (Sect. 3.1) and snow cover (Sect. 3.2).

3.1 Variation in albedo with increasing black carbon content in first year and multi-year sea ice

Figure 3 shows the diffuse albedo of the surface of the first year and multi-year sea ice with additional black carbon, in a top 5 cm layer, ranging between 1 and 1024 ng g^{-1} at wavelengths 400–700 nm. For both sea ice types as black carbon content increases the albedo decreases, with an albedo decrease to 98.7 % of the initial value for a black carbon increase from 1 to 8 ng g^{-1} in first year sea ice, and an albedo decrease to 99.6 % of the initial value in the multi-year sea ice for the same black carbon mass ratio increase. Thus the albedo of first year sea ice is more sensitive to additional black carbon than the multi-year ice.

The decrease in albedo with increasing mass ratio of black carbon is non-linear, for example, in the first-year ice (Fig. 3a) a doubling of additional black carbon from

2 to 4 ng g^{-1} leads to an albedo decrease to 99.7 % of the albedo value at 2 ng g^{-1}, but a doubling of additional black carbon from 512 to 1024 ng g^{-1} results in an albedo decrease to ∼ 64 % of the albedo value at 512 ng g^{-1}. While with the multi-year ice (Fig. 3b) a doubling of black carbon from 2 to 4 ng g^{-1} leads to an albedo decrease to 99.9 %, but a doubling from 512 to 1024 ng g^{-1} leads to an albedo decrease to ∼ 80 % at a wavelength of 500 nm. As the amount of black carbon increases the wavelength dependence of the albedo decreases, similar behaviour has been observed and explained in snow packs (Reay et al., 2012).

3.2 Effect of snow cover and type on the influence of black carbon in sea ice on surface albedo

Figure 4 shows surface albedo, with snow cover between 0 and 10 cm (1 m optically thick snow is also shown for comparative purposes), as a function of additional mass ratio of black carbon in sea ice at a wavelength of 500 nm. Two results are immediately obvious from Fig. 4. The addition of a thin layer (0.5 cm) of snow on sea ice can drastically increase the albedo of the surface, this is not a surprising result and has been suggested by Brandt et al. (2005). Secondly, the effect of a layer of snow in mitigating the albedo response of black carbon in sea ice is quantified for the first time. A layer of 2–5 cm of snow is effectively enough to mask any change in albedo owing to additional black carbon in sea ice. However whilst 2–5 cm of snow cover is enough to mask any change in additional black carbon in the sea ice it is not thick enough to be wholly responsible for surface albedo. The *e*-folding depths of the wet and dry snow pack are 12 cm and 6 cm at a wavelength of 500 nm and previously it has been shown that a snowpack needs to be greater than 3–4 *e*-folding depths before it is optically thick enough to be uninfluenced by the underlying layer (e.g. France et al., 2011).

Figure 4 shows dry snow has a much greater impact on mitigating the effect of black carbon in sea ice on surface albedo than wet snow; most noticeably observed with the addition of just a 0.5 cm layer of snow. With an increase in snow thickness from

5 to 10 cm of dry snow there is only a very small difference in albedo observed, with the same wet snow addition there is still a noticeable difference in albedo measured, suggesting a greater thickness of wet snow would be required for the snow layer to be optically thick. The increase in surface albedo owing to the addition of snow to sea ice is greater for the first year ice than the multi-year ice. The initial albedo of the first year ice is lower than the albedo of the multi-year ice and therefore a larger change in albedo occurs with addition of snow.

4 Discussion

The following discussion will focus on the light absorbing impurities in the sea ice, the response of albedo to black carbon depending on sea ice type, the effect of snow cover and finishes with a discussion on the limitations and future possibilities of the study.

4.1 Absorption cross-sections of snow and sea ice

Figure 2 shows the absorption cross-sections for the light absorbing impurities in the snow and sea ice types determined from the albedo and extinction coefficient data of Grenfell and Maykut (1977). Figure 2 shows variation with wavelength to be reasonably flat, but with a slight increase with longer wavelengths, this may be interpreted as consistent with a black carbon absorber as black carbon absorption is relatively flat within a wavelength range 400–700 nm as shown in Light et al. (1998, Fig. 13a).

From the typical absorption cross-sections in Fig. 2, from 400–600 nm, the mass ratio of black carbon in each sea ice/snow can be estimated using Eq. (3)

$$[\mathrm{BC}] = \frac{\sigma^{+}_{\mathrm{abs}}}{\sigma_{\mathrm{BC}}}, \tag{3}$$

where σ^{+}_{abs} is the average absorption cross-section over 400–600 nm in Fig. 2, σ_{BC} is the absorption cross-section for black carbon ($10\,m^2\,g^{-1}$), and [BC] is the black carbon mass ratio.

The granular white ice has an estimated equivalent black carbon mass ratio of $48\,ng\,g^{-1}$, the blue sea ice has $11.1\,ng\,g^{-1}$, the wet snow has $63\,ng\,g^{-1}$ and the dry snow has $83\,ng\,g^{-1}$. Although not improbable, these values are large compared to most previous literature reporting black carbon values in snow and sea ice. Clarke and Noone (1985) report typical Arctic black carbon in snow values ranging from $23\,ng\,g^{-1}$ at Barrow, Alaska, to $45.5\,ng\,g^{-1}$ at Alert, Canada. Grenfell et al. (2002) report average black carbon values in Arctic sea ice of $5.5\,ng\,g^{-1}$. Figure 6c of Warren and Wiscombe (1980) shows they required $300\,ng\,g^{-1}$ of black carbon to reproduce the albedo of the snow presented by Grenfell and Maykut (1977), and suggest that the large values of mass ratio of black carbon may be due to pollution from the T3 camp where measurements on the snow were taken. Note 3 on page 2732 of Warren and Wiscombe (1980) suggests that a value of $150\,ng\,g^{-1}$ is actually more accurate based on a more realistic density of the black carbon absorber. The mass ratio of black carbon in the snow presented by Warren and Wiscombe (1980) is still approximately twice those values presented here. To reconcile the different values of black carbon requires comparison of the two techniques of determining black carbon mass ratio. The calculations presented here use the same optical properties of the black carbon as note 3 in Warren and Wiscombe (1980) and further adopted by Warren (1982). The radiative-transfer calculations of Warren and Wiscombe (1980) reproduce the albedo data of Grenfell and Maykut (1977) only, whereas the work presented here reproduces the albedo and light penetration data. The work of Warren and Wiscombe (1980) requires an assumption of grain size based on absorption only by ice at a wavelength of 900 nm, and apparently assume no absorption by impurity at 900 nm, whereas the radiative-transfer calculation employed here requires no knowledge of the grain size. Thus the radiative-transfer calculation here may be a truer representation of the equivalent mass ratio of

black carbon as it is more constrained by experimental data, reproduces albedo and light penetration data and does not require assumption of grain size.

In the work presented here it is likely that not all absorption by light absorbing impurities is due to black carbon, and another light absorbing impurity is present. The presence of other light absorbing impurities could explain the increase observed with wavelength. Other light absorbing impurities present in sea ice and snow could include sediments, atmospheric dust, algae and HULIS (e.g. Light et al., 1998; France et al., 2012). France et al. (2012) suggest algae as a possibility for the increase in absorption observed at longer wavelengths. Light et al. (1998, Fig. 13a) and Perovich (2009, Fig. 3.6.2) show how ice algae absorption increases at wavelengths 600–650 nm. However ice algae absorption also peaks at wavelengths from 400–500 nm and decreases from 650–700 nm; trends that are not seen in the absorption cross-section in Fig. 2. The absorption of sediments and atmospheric dust are also shown in Light et al. (1998, Fig. 13a) and Perovich (2009, Fig. 3.6.2), (where atmospheric dust is assumed to have identical optical properties to sediments) these steadily increase from 550–700 nm, and therefore it is likely that there may also be sediment or dust in the snow and sea ice studied.

4.2 Variation in the impact of black carbon with sea ice type

Figure 3 surprisingly shows that the albedo of the sea ice surface is insensitive to *additional* black carbon mass ratios under $100\,ng\,g^{-1}$ added in the top 5 cm of the sea ice. It should be stressed that it is *additional* black carbon to that black carbon already present and the albedo of the sea ice is sensitive to absolute changes in black carbon mixing ratios of $1–100\,ng\,g^{-1}$. Figure 3 also shows that the impact of additional black carbon on surface albedo is dependant on the sea ice type, with the first year ice showing a much more sensitive response to black carbon than the multi-year ice. The multi-year ice consists of the granular white ice on top of a blue ice, while the first year ice is just the blue ice. The granular white ice has larger values for the scattering and absorption cross-sections than the blue ice.

Similar differences in the effect of black carbon on surface albedo with sea ice type are observed in previous modelling of black carbon in sea ice. Light et al. (1998) used a structural-optical model in combination with a four-stream radiative-transfer model to calculate the effects of increased soot concentration in a multi-year frozen sea ice, suggesting an increase from 0 to 100 ng g^{-1} of black carbon in the sea ice will decrease albedo to 73 % of the original value at 500 nm. While Grenfell et al. (2002) utilised a multilayer four-stream radiative-transfer model to investigate effects of varying concentrations and vertical distribution of soot on albedo, transmissivity, and internal heating of the ice, only reporting an albedo decrease to 99 % of the original value for a 0 to 100 ng g^{-1} black carbon increase in the top 1 cm layer of their sea ice. While calculations presented here suggest an albedo decrease to 96 % for multi-year ice and 91 % for first year ice for an additional black carbon increase of 100 ng g^{-1}. The greatest albedo difference is therefore observed by Light et al. (1998) who model a sea ice with scattering cross section values of 0.654, 1.46, 0.96 m^2 kg^{-1} in three layers from the top, 0.05, 0.2, 2.6 m thick respectively. These values compare with a scattering cross-section used by Grenfell et al. (2002) of 0.3 m^2 kg^{-1} in the upper 4 cm, with the lower 150 cm with a scattering cross-section of 0.0375 m^2 kg^{-1}. Compared to the scattering cross-sections used for our work of 0.03 m^2 kg^{-1} for first year sea ice and 0.87 m^2 kg^{-1} for the multi-year sea ice. The scattering cross-section and corresponding change in albedo implies a large value of the scattering cross-section will result in black carbon having less effect on surface albedo. Warren (1982) explains that a more scattering medium has a smaller grain size, and therefore more ice-air transitions, which are the most efficient location for photons to be scattered, while a photon only has chance of being absorbed as it passes through ice, where it can be absorbed by the ice matrix or by black carbon.

4.3 The role of snow and snow type in the influence of black carbon in sea ice on surface albedo

To the authors knowledge previous research into the effects of black carbon on surface albedo in sea ice has assumed snow free conditions typical of late and early periods in the sea ice season, e.g. Light et al. (1998) mention their study only being valid during the ablation season when snow cover is eliminated. Sea ice is predominately snow covered, Fig. 4 demonstrates the extent even a thin snow cover (< 1 cm) can diminish the effect black carbon in the sea ice has on the surface albedo. Figure 4 demonstrates that additional black carbon in the sea ice changes the surface albedo with up to 5 cm of snow and the snow is not optically thick until the snow is over 10 cm thick. Where optically thick is classed as when the surface albedo is no longer effected by further snow depth increments. France et al. (2011) state optically thick was typically when the snow thickness is 3–4 *e*-folding depths but for snow on sea ice a practical definition of optically thick appears to be approximately one *e*-folding depth of snow. The difference can be rationalised as optically thick for land based snowpacks occurs where there is no change in surface albedo with increasing snow thickness owing to influence of a dark ground surface, whereas for snow on sea ice the albedo difference between snow and sea ice is much smaller than for dark soil and snow. Albedo of optically thick snow (1 m thick) is also shown on Fig. 4 for comparison. Brandt et al. (2005) suggest from their results studying albedo of Antarctic sea ice that a snow covering of just 3 cm, or in some cases just 1 cm, can be classed as optically thick snow. The results presented here agree that a thin snow covering will greatly increase albedo but a snow cover greater than 3 cm would be needed to be described as optically thick.

Figure 4 also shows how the influence of black carbon in sea ice on surface albedo is effected by the type of snow cover. Dry snow has a greater effect at mitigating the impact of black carbon in sea ice on surface albedo, compared to the wet snow. The dry snow is a more scattering medium per unit depth evidenced by the *e*-folding depths given in Table 2. Therefore a smaller depth is required to be optically thick.

To understand the degree to which black carbon in sea ice may affect surface albedo knowledge of snow depth over sea ice and its variation seasonally and spatially is essential. Snow depth measurements over sea ice have been reported both from ground measurements (e.g. Warren et al., 1999; Massom et al., 2001) and more recently through satellite and airborne measurements (e.g Kanagaratnam et al., 2007; Kwok and Cunningham, 2008; Kwok et al., 2011; Galin et al., 2012). Two studies provide an overview of snow thicknesses over sea ice. Warren et al. (1999) present a comprehensive data set of Arctic Ocean snow cover from measurements of snow depth and density over 37 yr at the Soviet drifting stations, while Massom et al. (2001) using data collected over 10 yr, review snow thickness and snow type of Antarctic snow on sea ice. Arctic sea ice is mostly free of snow during the second half of July and all of August. Therefore during these months black carbon in sea ice would affect surface albedo. Snow thickness reaches a maximum in the Arctic in May when the average depth is 34.4 cm (Warren et al., 1999). In Antarctica mean snow thickness varies both seasonally and regionally due to differences in precipitation regimes and the age of the underlying ice (Massom et al., 2001). In March, in East Antarctica, 20 % of the sea ice is predominately snow free, and less than 10 % of the snow cover is thicker than 10 cm, by August (winter), snow thickness is typically 10–20 cm, but 10 % of the sea ice remains snow free (Massom et al., 2001). Therefore although snow on sea ice would appear to predominately mask the effects of black carbon in sea ice in both the Antarctic and Arctic, the effect of black carbon on albedo of sea ice is important for a couple of months of the year, in both the Antarctic and Arctic. These months would be following a period of snow melt over sea ice where black carbon may be concentrated onto the sea ice surface from meltwater (Grenfell et al., 2002). Doherty et al. (2010) measured spatial variation of black carbon through sea ice cores taken on sea ice in the southern Canadian basin suggesting black carbon is concentrated near the surface following snowmelt. However, further work on the distribution of black carbon in sea ice would be useful. The months would also coincide with higher surface irradiances owing to

smaller solar zenith angles, so melting may be exacerbated, as black carbon is able to absorb more radiation.

4.4 Potential limitations in the model and future research possibilities

In the results presented here there are several limitations; the method for obtaining scattering and absorption cross-sections, the absorption spectra of black carbon used and black carbon characteristics.

There is a source of uncertainty in the method for obtaining the absorption and scattering cross-sections from *e*-folding depth and albedo data (e.g. Lee-Taylor and Madronich, 2002; King et al., 2005; France et al., 2011, 2012). Figure 2 has error bars for the calculated values of absorption cross-section for light absorbing impurities, and Table 1 shows estimates of uncertainty for the calculated scattering values. These values of uncertainty were calculated through making small changes to the fit of the albedo and extinction coefficient data from Grenfell and Maykut (1977), and judged by eye, to ascertain how small changes affect the derived scattering and absorption values. All values of scattering cross-section are within 13 % of the reported value and the majority of absorption values are within 10 % of the reported value. Figure 5 shows a comparison between our modelled albedo and the original albedo measured by Grenfell and Maykut (1977) for each snow and sea ice type. A good fit between the albedo for each snow/sea ice type is observed, with all modelled albedo being within 10 % of the measured value and the two snows being within 2 % of the measured albedo.

The calculation to obtain values of the scattering and absorption cross-sections assumes all light absorbing impurities are due to black carbon. In reality impurities are likely to include other substances, for example HULIS, dust, sediment and marine algae that would contribute to absorption in the sea ice. The very strong absorption cross-section of black carbon compared to other substances often results in black carbon being the dominant absorbing impurity. The black carbon properties used for our calculations (refractive index, size and density) are taken to be a standard proxy for black carbon and are based on calculations by Warren and Wiscombe (1980, 1985).

Bohren (1986) reviewed uncertainties in the black carbon "constant" suggesting three main limitations. Bohren (1986) suggest it is unlikely all soot particles are spherical, as assumed, with different shaped particles potentially having different absorption efficiencies, e.g. plate-like particles would have an absorption cross-section twice as large as spherical particles. Secondly the refractive index utilised by Warren and Wiscombe (1980) ($1.8 + 0.5i$), has a factor of 5 uncertainty in the imaginary part (Roessler and Faxvog, 1980). Lastly the particle porosity is unknown and porous particles will be more absorbent than solid particles. The density of black carbon particles is discussed in Warren and Wiscombe (1985). France et al. (2012) recently demonstrated a good correlation between their black carbon absorption cross-section (used in this study) and the experimentally measured absorption cross-section of black carbon reviewed by Bond and Bergstrom (2006).

5 Conclusions

Absorption and scattering cross-section coefficients were calculated for a typical first year and multi-year sea ice and dry and wet snow types suggesting black carbon is the dominating absorbing impurity. Estimated black carbon mass ratios for the sea ice and snow are larger than previously reported suggesting the presence of a secondary absorbing impurity which is likely to be atmospheric dust/sediment. Radiative-transfer calculations demonstrate sea ice albedo is surprisingly unresponsive to additional black carbon additions up to $100\,\mathrm{ng\,g^{-1}}$ with a decrease in albedo to 99.6 % of the original value of albedo due to an addition of $8\,\mathrm{ng\,g^{-1}}$ black carbon in first year sea ice compared to an albedo decrease to 98.7 % for the same black carbon mass ratio increase in multi-year ice, highlighting that the first year sea ice proved more responsive to black carbon additions. The first year sea ice is a less scattering environment than the multi-year sea ice and comparison with previous literature suggests a less scattering sea ice environment will be more responsive to additional black carbon. As sea ice is predominately snow covered the influence of an overlying snow cover at mitigating the effects

of black carbon in the sea ice surface layer was also investigated. A 0.5 cm layer of snow greatly diminishes the effect of black carbon on surface albedo, and a 2–5 cm layer (less than half the *e*-folding depth of snow) is enough to "mask" any change in surface albedo owing to additional black carbon in sea ice, but not thick enough to ignore the underlying sea ice. Although the effects of black carbon in sea ice are limited to when snow cover is below 2–5 cm, black carbon is still critical in the sea ice system because as soon as snow is thin enough for black carbon in the sea ice to affect surface albedo it will exacerbate snow melting leading to longer snow free conditions, and also greater sea ice melting. Furthermore the period of the year when sea ice is snow free coincides with the smallest solar zenith angles, i.e. when the solar radiation is greatest, so the influence of black carbon will be larger.

Acknowledgements. MDK thanks NERC for support under Grants NE/F004796/1 and NE/F010788/1. AAM is supported by a Thomas Holloway Fellowship.

References

Barry, R. G.: The parameterization of surface albedo for sea ice and its snow cover, Prog. Phys. Geog., 20, 63–79, 1996. 945

Beine, H. J., Amoroso, A., Dominé, F., King, M. D., Nardino, M., Ianniello, A., and France, J. L.: Surprisingly small HONO emissions from snow surfaces at Browning Pass, Antarctica, Atmos. Chem. Phys., 6, 2569–2580, doi:10.5194/acp-6-2569-2006, 2006. 951

Bohren, C.: Applicability of effective-medium theories to problems of scattering and absorption by nonhomogeneous atmospheric particles, J. Atmos. Sci., 43, 468–475, 1986. 961

Bond, T. C. and Bergstrom, R. W.: Light absorption by carbonaceous particles: an investigative review, Aerosol Sci. Tech., 40, 27–67, 2006. 961

Brandt, R., Warren, S., Worby, A., and Grenfell, T.: Surface albedo of the Antarctic sea ice zone, J. Climate, 18, 3606–3622, 2005. 945, 947, 953, 958

Chýlek, P. and Ramaswamy, V.: Albedo of soot-contaminated snow, J. Geophys. Res., 88, 837–843, 1983. 945

Clarke, A. and Noone, K.: Soot in the Arctic snowpack: a cause for perturbations in radiative transfer, Atmos. Environ., 19, 2045–2053, 1985. 945, 955

Curry, J., Schramm, J., and Ebert, E.: Sea ice-albedo climate feedback mechanism, J. Climate, 8, 240–247, 1995. 945

Dittmar, T.: The molecular level determination of black carbon in marine dissolved organic matter, Org. Geochem., 39, 396–407, 2008. 945

Doherty, S. J., Warren, S. G., Grenfell, T. C., Clarke, A. D., and Brandt, R. E.: Light-absorbing impurities in Arctic snow, Atmos. Chem. Phys., 10, 11647–11680, doi:10.5194/acp-10-11647-2010, 2010. 945, 959

Flanner, M., Zender, C., Randerson, J., and Rasch, P.: Present-day climate forcing and response from black carbon in snow, J. Geophys. Res, 112, D11202, doi:10.1029/2006JD008003, 2007. 945

France, J. and King, M.: Hydroxyl (OH) radical production rates in snowpacks from photolysis of hydrogen peroxide (H_2O_2) and nitrate (NO_3^-), Atmos. Environ., 41, 5502–5509, 2007. 951

France, J., King, M., and Lee-Taylor, J.: The importance of considering depth-resolved photochemistry in snow: a radiative-transfer study of NO_2 and OH production in Ny-Alesund (Svalbard) snowpacks, J. Glaciol., 56, 655–662, 2010a. 951

France, J., King, M., and MacArthur, A.: A photohabitable zone in the martian snowpack? A laboratory and radiative-transfer study of dusty water-ice snow, Icarus, 207, 133–139, 2010b. 951

France, J. L., King, M. D., Frey, M. M., Erbland, J., Picard, G., Preunkert, S., MacArthur, A., and Savarino, J.: Snow optical properties at Dome C (Concordia), Antarctica; implications for snow emissions and snow chemistry of reactive nitrogen, Atmos. Chem. Phys., 11, 9787–9801, doi:10.5194/acp-11-9787-2011, 2011. 947, 951, 952, 953, 958, 960

France, J. L., Reay, H. J., King, M. D., Voisin, D., Jacobi, H. W., Domine, F., Beine, H., Anastasio, C., MacArthur, A., and Lee-Taylor, J.: Hydroxyl radical and NO_x production rates, black carbon concentrations and light-absorbing impurities in snow from field measurements of light penetration and nadir reflectivity of onshore and offshore coastal Alaskan snow, J. Geophys. Res., 117, 5502–5509, 2012. 951, 952, 956, 960, 961

Galin, N., Worby, A., Markus, T., Leuschen, C., and Gogineni, P.: Validation of airborne FMCW radar measurements of snow thickness over sea ice in Antarctica, IEEE T. Geosci. Remote, 50, 3–12, 2012. 959

Gardner, A.: A review of snow and ice albedo and the development of a new physically based broadband albedo parameterization, J. Geophys. Res., 115, F01009, doi:10.1029/2009JF001444, 2010. 945

Goldenson, N., Doherty, S. J., Bitz, C. M., Holland, M. M., Light, B., and Conley, A. J.: Arctic climate response to forcing from light-absorbing particles in snow and sea ice in CESM, Atmos. Chem. Phys., 12, 7903–7920, doi:10.5194/acp-12-7903-2012, 2012. 946

Grenfell, T. and Maykut, G.: The optical properties of ice and snow in the Arctic Basin, J. Glaciol., 18, 445–462, 1977. 946, 948, 949, 951, 954, 955, 960, 968, 973

Grenfell, T., Light, B., and Sturm, M.: Spatial distribution and radiative effects of soot in the snow and sea ice during the SHEBA experiment: the surface heat budget of arctic ocen (SHEBA), J. Geophys. Res., 107, 8032, doi:10.1029/2000JC000414, 2002. 945, 946, 947, 955, 957, 959

Hansen, J. and Nazarenko, L.: Soot climate forcing via snow and ice albedos, P. Natl. Acad. Sci. USA, 101, 423–428, 2004. 945

Highwood, E. and Kinnersley, R.: When smoke gets in our eyes: the multiple impacts of atmospheric black carbon on climate, air quality and health, Environ. Int., 32, 560–566, 2006. 945

Holland, M. M., Bailey, D. A., Briegleb, B. P., Light, B., and Hunke, E.: Improved sea ice shortwave radiation physics in CCSM4: the impact of melt ponds and aerosols on Arctic sea ice, J. Climate, 25, 1413–1430, 2012. 946

Jacobson, M.: Strong radiative heating due to the mixing state of black carbon in atmospheric aerosols, Nature, 409, 695–697, 2001. 945

Jacobson, M.: Climate response of fossil fuel and biofuel soot, accounting for soot's feedback to snow and sea ice albedo and emissivity, J. Geophys. Res., 109, D21201, doi:10.1029/2004JD004945, 2004. 946, 947

Kanagaratnam, P., Markus, T., Lytle, V., Heavey, B., Jansen, P., Prescott, G., and Gogineni, S. P.: Ultrawideband radar measurements of thickness of snow over sea ice, IEEE T. Geosci. Remote, 45, 2715–2724, 2007. 959

King, M. and Simpson, W.: Extinction of UV radiation in Arctic snow at Alert, Canada (82° N), J. Geophys. Res., 106, 499–12, 2001. 947

King, M., France, J., Fisher, F., and Beine, H.: Measurement and modelling of UV radiation penetration and photolysis rates of nitrate and hydrogen peroxide in Antarctic sea ice: an

estimate of the production rate of hydroxyl radicals in first-year sea ice, J. Photoch. Photobio. A, 176, 39–49, 2005. 947, 951, 952, 960

Kwok, R. and Cunningham, G. F.: ICESat over Arctic sea ice: estimation of snow depth and ice thickness, J. Geophys. Res., 113, C08010, doi:10.1029/2008JC004753, 2008. 959

Kwok, R., Panzer, B., Leuschen, C., Pang, S., Markus, T., Holt, B., and Gogineni, S.: Airborne surveys of snow depth over Arctic sea ice, J. Geophys. Res., 116, C11018, doi:10.1029/2011JC007371, 2011. 959

Ledley, T. S. and Thompson, S. L.: Potential effect of nuclear war smokefall on sea ice, Climatic Change, 8, 155–171, 1986. 945, 946

Lee-Taylor, J. and Madronich, S.: Calculation of actinic fluxes with a coupled atmosphere-snow radiative transfer model, J. Geophys. Res, 107, 4796, doi:10.1029/2002JD002084, 2002. 948, 950, 951, 952, 960

Light, B., Eicken, H., Maykut, G., and Grenfell, T.: The effect of included particulates on the spectral albedo of sea ice, J. Geophys. Res., 103, 27739–27752, 1998. 945, 946, 947, 954, 956, 957, 958

Light, B., Grenfell, T., and Perovich, D.: Transmission and absorption of solar radiation by Arctic sea ice during the melt season, J. Geophys. Res, 113, C03023, doi:10.1029/2006JC003977, 2008. 946

Masiello, C.: Black carbon in deep-sea sediments, Science, 280, 1911–1913, 1998. 945

Massom, R., Eicken, H., Hass, C., and Jeffries, M.: Snow on Antarctic sea ice, Rev. Geophys., 39, 413–445, 2001. 959

Middelburg, J. and Nieuwenhuize, J.: Black carbon in marine sediments, Mar. Chem., 65, 245–252, 1999. 945

Mitchell, M.: Visual range in the polar regions with particular reference to the Alaskan Arctic, J. Atmos. Terr. Phys., Special supplement 1, 195–211, 1957. 945

Perovich, D.: Complex yet translucent: the optical properties of sea ice, Physica B, 338, 107–114, 2003. 946, 947

Perovich, D.: The interaction of ultraviolet light with Arctic sea ice during SHEBA, Ann. Glaciol., 44, 47–52, 2006. 946

Perovich, D.: Sea ice optics measurements, in: Field Techniques for Sea Ice Research, edited by: Eicken, H., Gradinger, R., Salganek, M., Shirasawa, K., Perovich, D., and Lepparanta, M., University of Alaska Press, 2009. 956

Perovich, D. K. and Polashenski, C.: Albedo evolution of seasonal Arctic sea ice, Geophys. Res. Lett., 39, L08501, doi:10.1029/2012GL051432, 2012. 945

Perovich, D., Roesler, C., and Pegau, W.: Variability in Arctic sea ice optical properties, J. Geophys. Res., 103, 1193–1208, 1998. 946

Perovich, D., Grenfell, T., Light, B., and Hobbs, P.: Seasonal evolution of the albedo of multiyear Arctic sea ice, J. Geophys. Res., 107, 8044, doi:10.1029/2000JC000438, 2002. 945, 946

Phillips, G.: Verification of snowpack radiation transfer models using actinometry, J. Geophys. Res., 110, D08306, doi:10.1029/2004JD005552, 2005. 951

Ramanathan, V. and Carmichael, G.: Global and regional climate changes due to black carbon, Nat. Geosci., 1, 221–227, 2008. 945

Reay, H. J., France, J. L., and King, M. D.: Decreased albedo, *e*-folding depth and photolytic OH radical and NO_2 production with increasing black carbon content in Arctic snow, J. Geophys. Res., 117, D00R20, doi:10.1029/2011JD016630, 2012. 945, 953

Roessler, D. M. and Faxvog, F. R.: Optical properties of agglomerated acetylene smoke particles at 0.5145-µm and 10.6-µm wavelengths, J. Opt. Soc. Am., 70, 230–235, 1980. 961

Solomon, S., Qin, D., Manning, M., Chen, Z., Marquis, M., Averyt, K., Tignor, M., and Miller, H.: IPCC, 2007: Climate Change 2007: The Physical Science Basis. Contribution of Working Group I to the Fourth Assessment, Report of the Intergovernmental Panel on Climate Change, in: IPCC, 2007: Climate Change 2007: The Physical Science Basis. Contribution of Working Group I to the Fourth Assessment, Report of the Intergovernmental Panel on Climate Change, Cambridge University Press, 2007. 945

Stamnes, K., Tsay, S., Jayaweera, K., and Wiscombe, W.: Numerically stable algorithm for discrete-ordinate-method radiative transfer in multiple scattering and emitting layered media, Appl. Optics, 27, 2502–2509, 1988. 948

Suman, D., Kuhlbusch, T., and Lim, B.: Sediment Records of Biomass Burning and Global Change, Springer-Verlag, Berlin, 1997. 945

Warren, S.: Optical properties of snow, Rev. Geophys., 20, 67–89, 1982. 955, 957

Warren, S. and Brandt, R.: Optical constants of ice from the ultraviolet to the microwave: a revised compilation, J. Geophys. Res, 113, D14220, doi:10.1029/2007JD009744, 2008. 950

Warren, S. and Clarke, A.: Soot in the atmosphere and snow surface of Antarctica, J. Geophys. Res., 95, 1811–1816, 1990. 945

Warren, S. and Wiscombe, W.: A model for the spectral albedo of snow. II: Snow containing atmospheric aerosols, J. Atmos. Sci., 37, 2734–2745, 1980. 947, 950, 955, 960, 961

Warren, S. and Wiscombe, W.: Dirty snow after nuclear war, Nature, 313, 467–470, 1985. 945, 950, 960, 961
Warren, S., Rigor, I., Untersteiner, N., Radionov, V., Bryazgin, N., Aleksandrov, Y., and Colony, R.: Snow depth on Arctic sea ice, J. Climate, 12, 1814–1829, 1999. 959
Warren, S. G.: Impurities in snow: effects on albedo and snowmelt, Ann. Glaciol., 5, 177–179, 1984. 945
Weeks, W.: On Sea Ice, University of Alaska Press, 2010. 947

Table 1. Properties and measurement conditions of the snow and sea ice used in the study presented here. Measurement date, sky conditions, solar zenith angle, density, albedo and extinction coefficient are all from (Grenfell and Maykut, 1977). The values of the scattering cross-sections are calculated from the albedo and extinction coefficient data.

Snow/sea ice Type	Measurement date	Sky conditions	Solar Zenith angle/°	Density/ g cm^{-3}	Figure (Albedo)	Figure (Extinction Coefficient)	Maximum *e*-folding depth/cm	Asymmetry Parameter (g)	Scattering Cross-Section (σ_{scatt})/ m^2 kg^{-1}
Blue Sea Ice	15 Jun 1972	Clear	50	0.9	2d	3e	1.22	0.95	0.03 ± 0.003
Granular White Sea Ice	1 Jul 1974	Clear	65	0.5	2b	3c	0.31	0.95	0.87 ± 0.079
Dry Snow	20 Jun 1972	Clear	50	0.4	1a	3a	0.06	0.89	8.35 ± 1.09
Wet Snow	20 Jun 1972	Diffuse	50	0.47	1b	3b	0.12	0.89	1.99 ± 0.23

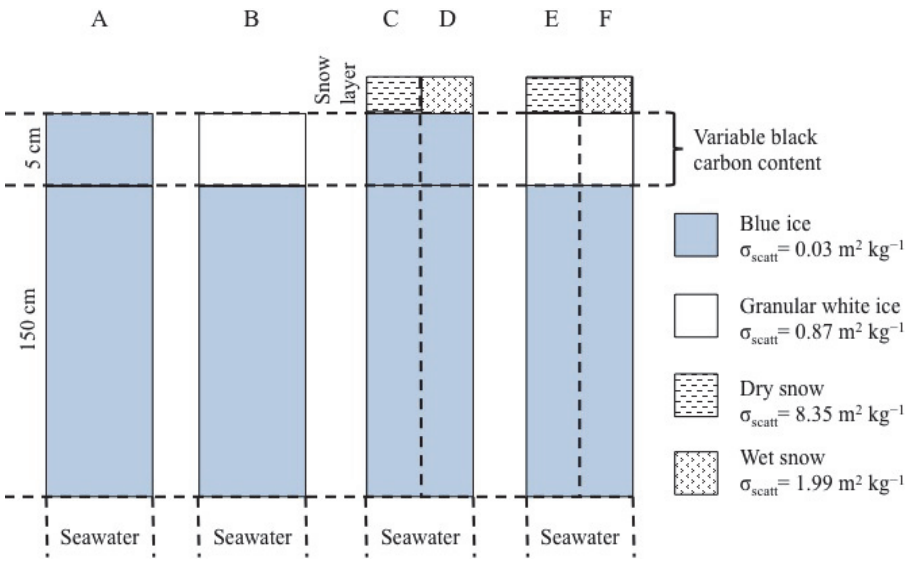

Fig. 1. Sea ice and snow configurations modelled (not to scale).

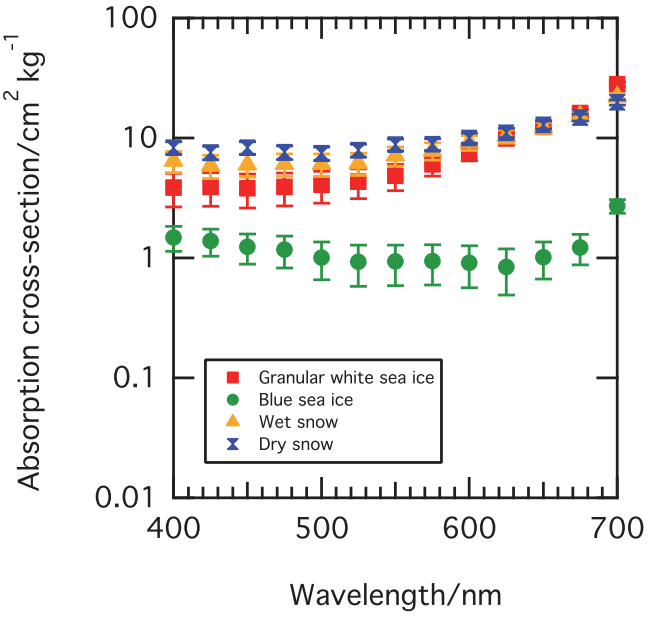

Fig. 2. Comparison of calculated absorption cross-sections ($\sigma^{+}_{abs}(\lambda)$) for granular white ice, blue ice, wet snow and dry snow. The absorption cross-sections for granular white sea ice and blue sea ice include absorption by ice, brine and impurties, while absorption in the wet and dry snow is by ice and impurities. Impurities are all assumed to be black carbon. Error bars show the average difference in calculated absorption values through making small changes to the data fit for obtaining these values.

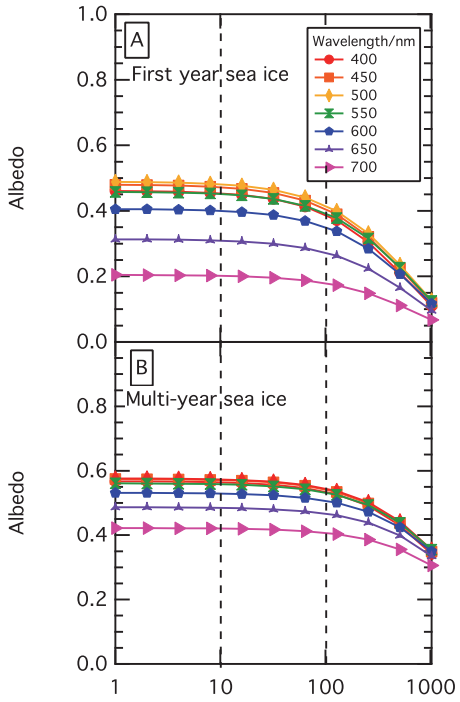

Fig. 3. (A) Albedo with increasing black carbon content from 1–1024 ng g^{-1}, evenly distributed in the top 5 cm of 155 cm of typical first year ice. **(B)** Albedo with increasing black carbon content from 1–1024 ng g^{-1}, evenly distributed in the top 5 cm of a typical multi-year ice.

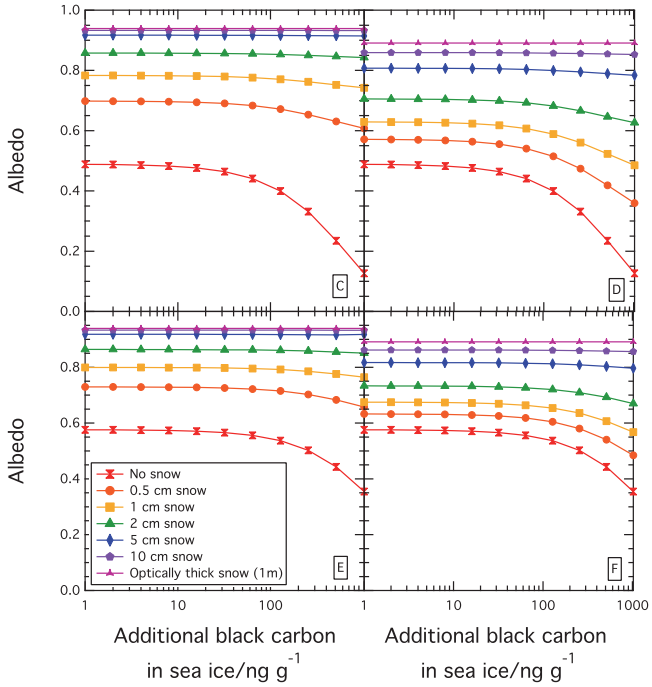

Fig. 4. Albedo of snow surface at 500 nm with different thicknesses of snow cover overlying sea ice. **(C)** dry snow on first year ice, **(D)** wet snow on first year ice, **(E)** dry snow on the multi-year ice, **(F)** wet snow on multi-year ice.

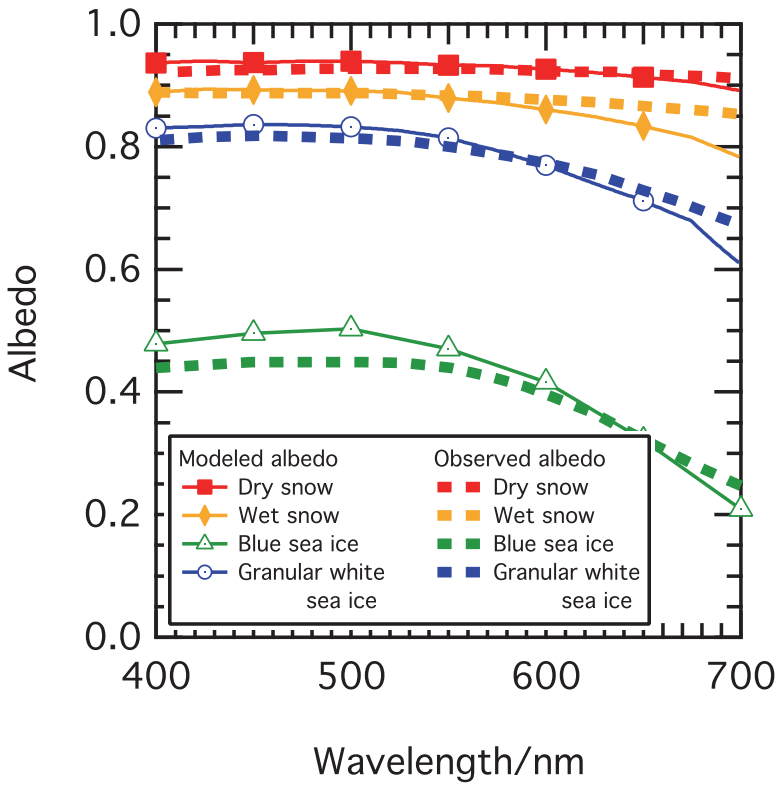

Fig. 5. Comparison of measured albedo by Grenfell and Maykut (1977) with albedo modeled by the TUV-snow model.